

Usak University

Journal of Engineering Sciences

An international e-journal published by the University of Usak

Journal homepage: dergipark.org.tr/uujes



Research article

Mg/Zn COMPOSITES PRODUCED BY MECHANICAL ALLOYING AND HOT PRESSING AND IN-VITRO BIODEGRADATION

Simay Erdibil^{1*}, Serap Cesur², Rasim İpek³

¹Ege University, Department of Material Science and Engineering, Izmir, Turkey

²Ege University, Engineering Faculty, Department of Chemical Engineering, Izmir, Turkey

³Ege University, Engineering Faculty, Department of Mechanical Engineering, Izmir, Turkey

Received: 18 Oct 2018

Revised: 26 April 2019

Accepted: 2 May 2019

Online available: 30 June 2019

Handling Editors: Eylem Kılıç, Kemal Mazanoğlu

Abstract

Biodegradable implants have many advantages over conventional steel and titanium based implants. Most important one of these advantages is the ability of these implants to degrade within a desired span of time (compatible with tissue and bone growth) after their function is over, without giving any harm to the body. The aim of this study is to develop a magnesium based biodegradable implant to be used as a bone plate. Mechanical and physical properties of Mg alloys that should possess for these applications are almost completely established, whereas the applicability still has to be investigated. In this study, Mg/MgZn/Zn composites were produced by mechanical alloying and hot pressing. Biodegradability of Mg/MgZn/Zn composites was tested as in-vitro in simulated body fluid (SBF) solution. SBF is nearly equal to human body blood plasma with ion concentrations. Seven implants were produced. They were placed in SBF solution and then their corrosion resistances were followed. During the process, visual changes of the implants were observed, pH, Mg ion concentrations of SBF solutions and mass, dimensional changes of degraded implants in solutions were measured. As soon as, implants were placed in SBF solutions, gas outlet of H₂ was observed, because of Redox reaction, which took place between implants and SBF. The composites in SBF remained between 1-360 hours and Zn% 2.35 and 3.10 had the longest degradation time when compared to others. Therefore, only three of the composites Zn% 0 (7h), 2.35 (360h) and 3.10 (192h) were selected for further, SEM and mechanical control tests.

Keywords: Magnesium; Zinc; MgZn composites; biodegradable implants; SBF.

©2019 Usak University all rights reserved.

1. Introduction

Magnesium alloys as light structural materials are widely used in aerospace, automobile and electronics industries [1,2].

*Corresponding author: Simay Erdibil (ORCID ID: 0000-0002-8687-5312)

E-mail: simayerdibil@gmail.com

Biodegradable implants have significant advantages over traditional steel and titanium based implant materials. They function in the body and then disintegrate in the desired time (in time compatible with tissue development) and do not harm the patient. The most investigated biodegradable material is Mg alloys. Biocompatible Magnesium and its alloys promise to be similar in terms of their mechanical properties to the target implant tissues (orthopedic tissues, jaws and teeth, stent, etc.) in the body [3,4].

After almost a century and a half of development, biodegradable magnesium implants, wires for the cardiovascular, musculoskeletal and ligature [5], and other designs, wires for the treatment of aneurysms [6], vascular stents [7] and osteosynthetics [8], bio batteries for pacemakers [9], manufacturers were widely used in surgery.

When the literature is examined, it is observed that the use of Mg-based alloys as 'intelligent implants' and their performance in in-vitro and in-vivo tests show a remarkable stage in the last 15 years [10-19].

The design criteria of the new generation implants, which can be bioactive in the human body and produced with materials with excellent biocompatibility and suitable corrosion and mechanical properties, are given in the literature [3,7,14,20]. The target is to produce a new generation of biodegradable Mg-based alloys with these properties. Mechanical and corrosion performances depend on the microstructure of alloy design, element selection, production process, heat treatment and alloying elements varying in the type and amount of the elements.

In this work, biodegradable Mg alloys will be developed. Mechanical alloying (MA) technique was chosen. Very fine-grained alloy powders are obtained. Solid-state chemical reactions can occur for the production during the process. Thus, materials with a wide variety of alloys, microstructures and properties can be produced. The mechanical alloyed powder mixture is shaped and sintered by powder metallurgy cold isostatic pressing (CIP). It will also be subjected to extrusion so that superior microstructure (controllable) can be obtained. After the production, the characterization tests are carried out.

The following objectives are expected to achieve in this study:

- i.* Develop biodegradable Mg alloy that the Mg removal rate (corrosion rate) should be less than 0.5 mm/year.
- ii.* Biodegradability can be determined / adjusted depending on alloy elements and processes (4-24 months).
- iii.* In terms of its mechanical properties, for orthopedic implants, it is required to be close to bone values and the values given in Table 1 are taken as basis.
- iv.* Managing the biodegradation process that conservation of integrity in the first 4 months.
- v.* Grain structure required is to be in fine-micro dimension.
- vi.* The porosity should be between 1% and 6%, depending on the above mechanical values and elongation ratio% (min 8%).
- vii.* Variables essential to implant design are mechanical expectancy, alloy ratios, grinding time, sintering time and how effective they are.

Table 1 Required mechanical properties for orthopedic implants [3].

| Material | Density (gr/cm³) | Elastic Modulus (GPa) | Compressive yield strength (MPa) | Fracture toughness (MPa^{1/2}) |
|---------------------------|--|--------------------------------------|---|---|
| Natural Bone | 1.8-2.1 | 3-20 | 110 | 3-6 |
| Biodegradable Mg Alloy | 1.74-2.0 | 41-45 | 200 | 15-40 |

Biodegradable implants are designed to provide temporary support during healing of diseased or damaged tissue, and to deteriorate without damaging to the tissue after control. The properties required are given below:

- It has biocompatibility and bioactivity.
- Biodegradation process: It depends on application area. Orthopedic applications should provide mechanical integrity that protects the bone for up to 12-18 weeks before bone tissue heals [3].
- Mechanical properties: It should not cause stress shielding, it should have high durability close to the bone and low modularity. For bone-based implants, the strength should be higher than 200 MPa and the elongation% should be more than 10% [14].
- Corrosion properties: Corrosion rate should be less than 0.5 mm/year in 37 °C simulated body fluid (SBF) [20].
- Tissue healing process: It must have blood-compatible and drug delivery capacity, as well as having adequate mechanical properties and rate of disruption [7].

When Mg is alloyed with Rare Earth Elements (RE), adequate research is available and still under investigation, in terms of strength, elastic modulus, corrosion resistance and biocompatibility, can be used to make biodegradable stents and implant screws [21].

The other important Mg alloys are Mg-Zn based alloys and this alloy is also effective in terms of corrosion rate. In addition to Zn and RE alloy elements, alloying elements such as Zr, Ca, Sn are also included in research to develop biodegradable implant materials.

In the research on Mg-based biodegradable implant development, the following areas are considered [21-23]:

- Variables of Mg-based alloys, alloy content, impurity, mode of production and microstructure, mechanical properties and their development.
- The development of the biocompatibility and mechanical integrity of Mg-based alloys formed with the vital elements (Ca, Zr, Sn and Sr) present in the human body.
- Managing the biological entities in the implant and tissue interface.
- Structural properties of magnesium alloy implants are porosity, surface state (ceramic and polymeric coatings), investigation of hybrid and composite structures [21,22,23].
- Improvement of drug delivery system performance or cell and tissue specific properties for tissue growth of implant [23].

1.1. Biodegradability principles of magnesium alloy development

The first principle in the selection of biodegradable Mg alloys is toxicity. In the disintegration process of alloys, the disinfecting product must be non-toxic and absorbable

by the environment of the skin or erythematous (in the kidneys). Elements according to these principles [16,24,25]:

- i. Known toxic elements: Ba, Be, Cd, Pb, Th
- ii. Elements that are likely to cause different allergic problems or hepatotoxicity in human: Al, Cr, V, Co, Ni, Ce, Cu, Pr
- iii. Vital elements in human body: Ca, Mn, Sn, Zn, Si
- iv. Vital elements found in plants and animals: Al, Li, Bi, Ag, Zr, Sr

Another criterion in alloy selection is the ability to increase the strength of the alloy [26,27]:

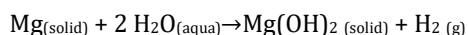
- i. Impurities: Fe, Ni, Cu, Co
- ii. Simultaneous development of durability and ductility; developers of durability: Al, Zn, Ag, Ca, Ce, Cu, Ni, Th; and elements that increase ductility: Th, Zn, Ag, Ca, Ce, Al, Ni, Cu
- iii. Magnesium has little effect on durability, elements developed for ductility: Cd, Li, Tl
- iv. Elements reducing ductility when magnesium is increasing in strength: Sn, Pb, Bi, Sb

Another criterion is the rate of corrosion. The electrochemical potentials of the alloying elements or magnesia (-2.37 V) can be improved by the intermetallic phase reducing internal galvanic corrosion at a similar potential. These elements: Y, -2.37 V; Nd, -2.43 V; and Ce, -2.48 V [3,28,29].

1.2. Corrosion rate

Although the potential for pure metals are provided by electrochemical potential series and the corrosion mechanism of magnesium is shown on the Pourbaix diagrams, the corrosion behaviors of multi-elemental Mg-based alloys are still difficult to predict. This is caused by micro galvanic corrosion in multi-elemental alloys that depends on the potential difference between intermetallic phases and the matrix [30].

The newly developed alloys' potentials are normally not available. The magnesium corrosion reaction in aqueous environment produces magnesium hydroxide and hydrogen gas:



Magnesium hydroxide may act as a corrosion protective layer in water. When the chloride concentration is above 30 mmol/ L, it starts to lose their facilities and convert into highly soluble magnesium chloride [22].

Hydrogen gas is a major element for using Mg-based alloys for orthopedic applications due to the bone vascularization that causes the formation of excessive hydrogen gas. Then, it results in potentially harmful gas pockets [31].

Although recent research has put forward that the hydrogen gas can be formed rapidly through the skin and accumulated in fatty tissue, hydrogen gas existing with implant application may not be of major concern. To develop new materials is better way for eliminating these problems. The major strategy is to develop metal glasses with high Zn content, particularly above the Zn-alloying threshold value [23].

The other solution is to increase the corrosion resistance of Mg-based alloys and to control hydrogen production. For this purpose, some processes have been recently developed to increase Magnesium corrosion resistance such as creating Mg-based alloys with different

elements, heat treatment process and surface modifications. The corrosion resistance and rate of Mg-based alloys can be improved in many ways. These methods are mentioned below.

Alloying: Mg alloys generally exhibit better corrosion resistance in living tissue (in-vivo) than in an artificial culture medium (in-vitro). In live animal model, disruption is investigated in the simulated body fluid (SBF), where disruption is generally higher. This is because of the static structure of the environment of the artificial culture medium and the dynamic structure of the living tissue environment. Other causes of the decay rate decrease are the protective effect of the corrosion layer formed immediately after the pH drop and [32-34];

- ✓ The protein coating on the surface of the implant in response to the initial operation in the living tissue environment [32].
- ✓ Mg-RE based biodegradable alloys generally exhibit better corrosion performance [33].
- ✓ Corrosion resistance of Mg-Zn based alloys not containing Rare Earth Element (RE) seems promising.
- ✓ The test of corrosion rates made in different environments can vary considerably [34].

Certain residues (impurities, Be, Fe, Ni and Cu) which adversely affect the corrosion resistance of magnesium and are frequently found in Mg alloys should be strictly controlled. These elements are harmful because of their low solubility in magnesium and Mg-based alloys forming corrosion cell (active cathodic) [31].

The presence of contaminants reduces the effect of other alloying elements, threatening the reactions and mechanical integrity of the alloying elements. Moreover, the faster degradation of the implant, the residues such as Ni and Cu, is caused by the toxic effect in the human body. For these reasons, the impurity in the alloy must not exceed a certain proportion. The range of acceptable levels for Be is 2 to 4 ppm by weight, Cu is 100-300 ppm, Fe is 30-50 ppm and Ni is 20-50 ppm [16]. It is stated that Mg-based biodegradable materials are more durable and ductile when they are in high purity [35]. Also, Zinc (Zn) has been shown to have a positive effect for eliminating the effects of elements such as Iron (Fe) and Nickel (Ni) which are toxic [15]. The addition of Manganese (Mn) to Mg-based alloys has also been shown to reduce the harmful effects of Iron (Fe) and increase the corrosion resistance [36].

2. Material and method

2.1. Material

Pure Magnesium: 99.2% pure and 150 μm particule diameter and Zn 97-99% pure and 150 μm particule size were used. The SBF (simulated body fluid) chemicals used in this work are NaCl, NaHCO_3 , KCl, NaHPO_4 , $\text{MgCl}_2 \cdot 6\text{H}_2\text{O}$, NaSO_4 , TBS, $\text{CaCl}_2 \cdot 2\text{H}_2\text{O}$, HCl 37%, supplied by Applichem and Merck. SBF were prepared in a polypropylene plastic material. The reactions that can occur with the glass surface in the SBF preparation process can disrupt the structure of the SBF solution.

2.2. Method

In this study, Mg implants as Zn% in Mg as 0%, 2.35%, 3.10%, 7.05%, 11.00%, 11.05% and 11.75% were prepared by hot pressing (sinter hot press HP15-3000) and compressive strength test (Autograph AG IS 100 kn) were performed. For preparing SBF solution, a sensitive scale, a magnetic stirrer, an ultrasonic bath, a pH meter (Hanna HI2002-02) and

a thermometer were used. The prepared SBF solution and samples were set at 37 °C. The ion concentrations of SBF solution prepared for in-vitro corrosion rate of these implants are given in Table 2.

Table 2 Comparison of ion concentration of human blood and SBF solution [20].

| Ion | Ion concentration(mM) | |
|--------------------------------|-----------------------|-------|
| | Blood Plasma | SBF |
| Na ⁺ | 142.0 | 142.0 |
| K ⁺ | 5.0 | 5.0 |
| Mg ²⁺ | 1.5 | 1.5 |
| Ca ²⁺ | 2.5 | 2.5 |
| Cl ⁻ | 103.0 | 147.8 |
| HCO ₃ ⁻ | 27.0 | 4.2 |
| HPO ₄ ²⁻ | 1.0 | 1.0 |
| SO ₄ ²⁻ | 0.5 | 0.5 |
| pH | 7.2-7.4 | 7.4 |

2.3. Preparation of Mg/Zn alloys

The Mg/Zn alloy samples prepared by atomised Mg and Zn powders with purity 99% and average grain size 63 µm were utilized. In this study, a mixture of Mg and Zn powder was prepared and with Zn content as 0%, 2.35%, 3.10%, 7.05%, 11.00%, 11.05% and 11.75% with the help of a V-blender by mixing for 1h. The Mg/Zn samples were then mechanically alloyed. The powders were planetary ball milled for 8 h using 10 mm-diameter stainless steel balls with weight ratio of 10:1 and rotating speed of 250 r/min. Then, high-strength graphite die with 10 mm in inner diameter and 60 mm in height was used as samples of sintering process. The ball milled powders were put into graphite die and sintered under pressure of 30 MPa (hot press) in argon atmosphere. It consists in heating the samples upto 420°C at a rate of 50 °C/min and holding at this temperature for 15 minutes.

2.3.1. Mechanical alloying

The mechanical alloying method is used to produce high strength composite materials with a finer and homogeneous microstructure by periodically welding (dry and) solid powders and breaking these welds again. In this method, the powders are placed in a closed vessel and the shaft is rotated. The powders are deformed by the help of shaft arms and balls, and in these dusts break and cold welds occur.

2.3.2. Hot pressing

Process steps are given as follows:

- Application of boron nitride to the surfaces of the mold
- Dust placement of molds
- Mold placement of the thermocouple
- Making pressure setting, contacting machine and mold surfaces
- Opening the vacuum after placing the lid
- Supply of argon gas to improve the vacuum environment
- Opening the heating
- Setting pressure value to desired value
- Waiting 15 minutes for sintering
- Closing the heating, the gas and vacuum
- Removing the sample from the mold

Sintering is performed at temperature between 450-470 °C.

2.3.3. Compressive Strength Test

External forces acting inward from the surface of the materials are called push forces and create pressure stresses. In the compression test, cylindrical or cubic specimens are placed between two parallel tables and the shape changes which are generated by the applied force are measured with the help of an extensometer.

2.4. Preparation of simulated body fluid

Since simulated body fluid (SBF) is supersaturated with respect to apatite, inappropriate preparation method can yield precipitation of apatite in solution. The prepared solution is kept transparent and colorless; and no deposit remains on the surface of bottle. If any precipitation occurs, the process of preparing SBF is stopped, the solution is abandoned, the process is restarted from washing the apparatus and SBF is prepared again. In order to prepare 1000 ml of SBF, first of all, 700 ml of ion-exchanged and distilled water is put with a stirring bar into 1000 ml plastic beaker. Then it is placed into the water bath on magnetic stirrer and covered with a plastic wrap or watch glass. The water in beaker is heated to $36.5 \pm 1.5^\circ\text{C}$ under stirring.

Only the reagents of 1st to 8th order are dissolved into the solution at $36.5 \pm 1.5^\circ\text{C}$ one by one in the order given in Table 2 by taking care of the indications in following list. The reagents of 9th (Tris) and 10th order (small amount of HCl) are dissolved in the following process of pH adjustment:

- i. To prepare SBF, glass containers must be avoided, but plastic containers with smooth surface (without any scratches) is suggested. Because, apatite nucleation can be excited at the glass container surface or at the edge of scratches. If the container is scratched, it is replaced by a new one.
- ii. Several reagents should not be dissolved simultaneously. A reagent is dissolved only after the preceding one (if any) completely dissolved.
- iii. The reagent CaCl_2 , which largely affects the precipitation of apatite, takes usually granular form and needs much duration to dissolve on granule. One is completely dissolved before initiation of dissolution of the next.
- iv. Volume of 1M-HCl is measured by cylinder after washing it with 1M-HCl. Hygroscopic reagents as KCl, $\text{K}_2\text{HPO}_4 \cdot 3\text{H}_2\text{O}$, $\text{MgCl}_2 \cdot 6\text{H}_2\text{O}$, CaCl_2 , Na_2SO_4 are also measured in a period as short as possible.
- v. The solution temperature is set as $36.5 \pm 1.5^\circ\text{C}$. If the amount of solution is smaller than 900 ml, ionexchanged is added and distilled water is increased to 900ml in total.
- vi. Electrode of the pH meter is inserted into the solution. The pH of solution should be 2.0 ± 1.0 just before dissolving the Tris.
- vii. The solution at preferably to $36.5 + 0.5^\circ\text{C}$ is prepared with the reagent Tris which is dissolved into the solution with carefully controlling the pH. At this stage, the amount of Tris and it's dissolving are very important to keep certain conditions. The pH value around $7.30 + 0.05$ must be also constant at $36.5 + 0.5^\circ\text{C}$ of the solution temperature.

Note 1: Adding Tris must be controlled and mixed into the solution under the certain control conditions, because the radical increase in local pH of the solution may lead to the precipitation of calcium phosphate. If the solution temperature is not within $36.5 \pm 0.5^\circ\text{C}$, add Tris to raise the pH to 7.30 ± 0.05 , stop adding it and wait for the solution temperature to reach $36.5 + 0.5^\circ\text{C}$.

Note 2: The pH value must be lower than 7.45 at 36.5 ± 0.5 °C, taking account of the pH decrease with increasing solution temperature (the pH value falls about $0.05/^\circ\text{C}$ at 36.5 ± 1.5 °C) [20].

3. Result and discussion

Mg/MgO implants with different Zn contents as 0%, 2.35%, 3.10%, 7.05%, 11.05% and 11.75% are placed into 20 ml of SBF solution in different beakers at 37 °C and changes of pH values by time are measured. Fig. 1 shows time-varying pH values of the SBF solution in which seven different implants are present.

The pH value of the implant with 11.75% Zn content at the end of the 1 hour was measured as approximately 10.5. The sharp increase of the pH value was also experimentally followed by deep slits in the sample, rapid H₂ gas output and turbidity in the solution. The implant with 11.75% Zn ratio was fragmented in H₂ at the end of 2 hours. In the 7th hour of the experiment, the Mg/MgO composite was completely disintegrated and the implant with 7.05% Zn ratio was divided into 3 parts. In the period upto the 23rd hour of the experiment, the implants with 11.00% and 11.05% Zn ratios were completely collapsed.

The implant with a ratio of 3.10% Zn showed a resistance of 192 hours with pH values between 8.0-9.5 and at the end it was divided into 2 parts. During this time, a white Mg (OH)₂ layer and a black precipitate layer were observed at the base of the SBF solution (as seen in Table 5) outside the implant. The sample with a ratio of 2.35% Zn showed 360 hours of resistance.

In Table 3, mass and size changes of all implants were examined. It can be seen that mass, height and diameter of the implants increase by time because of disintegration of the structure.

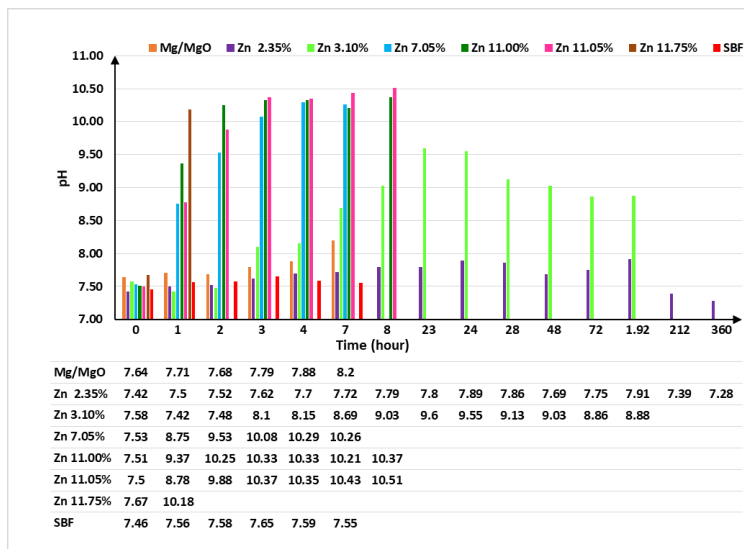


Fig. 1 Time-dependent pH value changes of SBF solutions containing implants.

The concentration of Mg ions in the SBF solution during the time that the implants remained was analyzed by Atomic Absorption Spectroscopy. This process was prepared by diluting the stock solution of 50 ppm to 1, 5, 10, 15 and 20 ppm. The absorbance values of the solution was measured to obtain the calibration graph shown in Fig. 2.

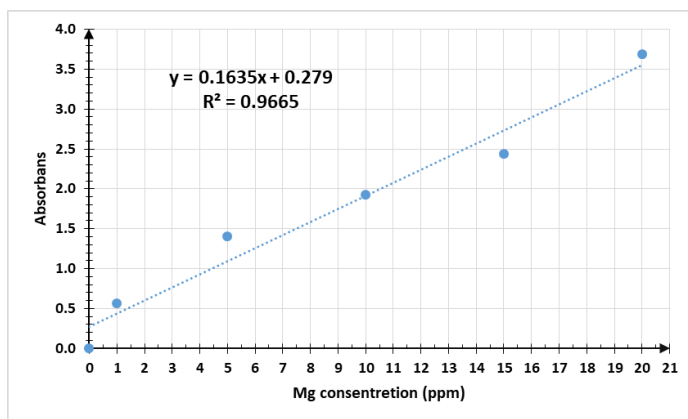


Fig. 2 Calibration graph.

The absorbance values of the implants in the individual SBF solution and the solution samples taken at changing time were analyzed by AAS and the values can be seen in Table 4. These values are obtained from the calibration curve (Fig. 2) and Mg ion concentration changes of implant containing SBF solutions are given Fig. 3. The 11.75% Zn ratio implant implies that the Mg concentration at the first hour is too high which shows high migration of Mg from the implant to the SBF solution, and thus the implant cannot maintain its strength in the SBF. This is also supported by pH values.

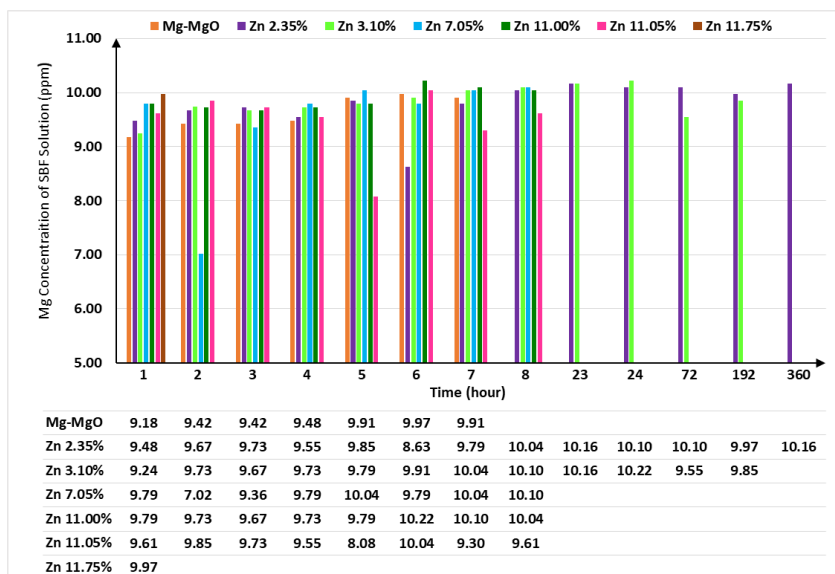


Fig. 3 Change in Mg ion concentration relative to time in SBF solutions containing implants.

The compression test applied to the Mg/MgO implant with 0% Zn ratio is given in Fig. 4. The compression test results of implants with 2.35% and 3.10% Zn ratios are given in Fig. 5 and Fig. 6, respectively.

Table 4 Absorbance values of Mg/Zn implants in SBF solution as a function of time by AAS.

| Time(h) | Mg implants with Zn content% | | | | | | |
|---------|------------------------------|------|------|------|-------|-------|-------|
| | Mg-MgO | 2.35 | 3.10 | 7.05 | 11.00 | 11.05 | 11.75 |
| 1 | 1.78 | 1.83 | 1.79 | 1.88 | 1.88 | 1.85 | 1.91 |
| 2 | 1.82 | 1.86 | 1.87 | 1.10 | 1.87 | 1.89 | |
| 3 | 1.82 | 1.87 | 1.86 | 1.81 | 1.86 | 1.87 | |
| 4 | 1.83 | 1.84 | 1.87 | 1.88 | 1.87 | 1.84 | |
| 5 | 1.90 | 1.89 | 1.88 | 1.92 | 1.88 | 1.60 | |
| 6 | 1.91 | 1.69 | 1.90 | 1.88 | 1.95 | 1.92 | |
| 7 | 1.90 | 1.88 | 1.92 | 1.92 | 1.93 | 1.80 | |
| 8 | | 1.92 | 1.93 | | 1.92 | 1.85 | |
| 23 | | 1.94 | 1.94 | | | | |
| 24 | | 1.93 | 1.95 | | | | |
| 72 | | 1.93 | 1.84 | | | | |
| 192 | | 1.91 | 1.89 | | | | |
| 360 | | 1.94 | | | | | |

In the compressive strength test, Mg/MgO composite with Zn of 0% (in Fig. 4) was subjected to deformation under 20.09 N/mm² force. The deformation occurred at 57.45 N/mm² force in the implant containing 2.35% Zn as given in Fig. 5. The force deformed with the 3.10% Zn ratio given in Fig. 6 was 61.64 N/mm². It has been observed that the sample having 3.10% Zn content is strongest one.

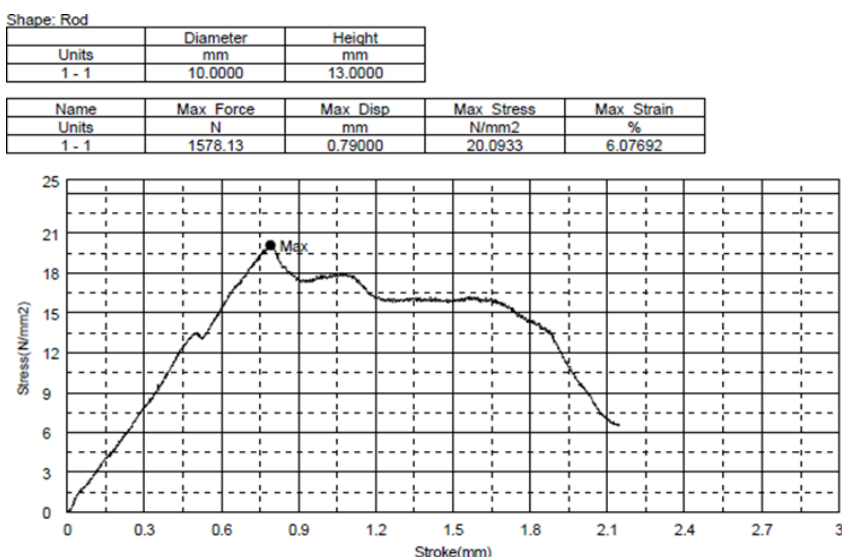


Fig. 4 Mg/Zn (0% Zn) Compression Strenght Test graph.

Shape: Rod

| | Diameter | Height |
|-------|----------|---------|
| Units | mm | mm |
| 1 - 1 | 10.0800 | 10.8800 |

| Name | Max Force | Max Disp | Max Stress | Max Strain |
|-------|-----------|----------|------------|------------|
| Units | N | mm | N/mm2 | % |
| 1 - 1 | 4584.38 | 2.77700 | 57.4473 | 25.5239 |

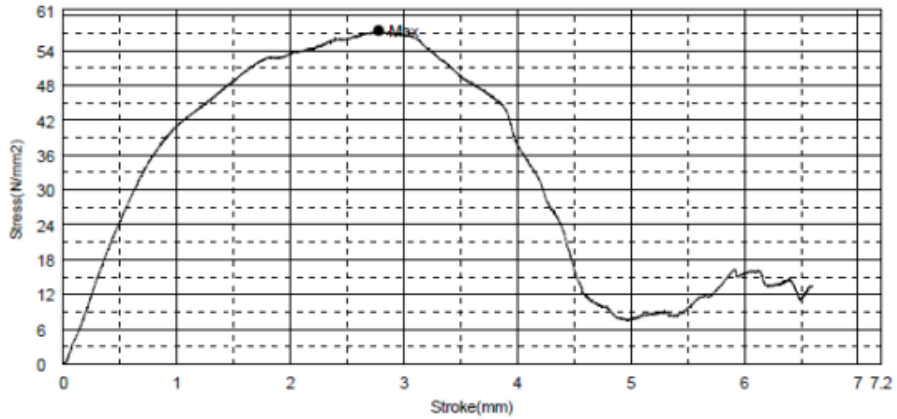


Fig. 5 Mg/Zn (2.35% Zn) Compression Strength Test graph.

Shape: Rod

| | Diameter | Height |
|-------|----------|---------|
| Units | mm | mm |
| 1 - 1 | 9.9700 | 11.8500 |

| Name | Max Force | Max Disp | Max Stress | Max Strain |
|-------|-----------|----------|------------|------------|
| Units | N | mm | N/mm2 | % |
| 1 - 1 | 4812.50 | 2.98800 | 61.6440 | 25.2152 |

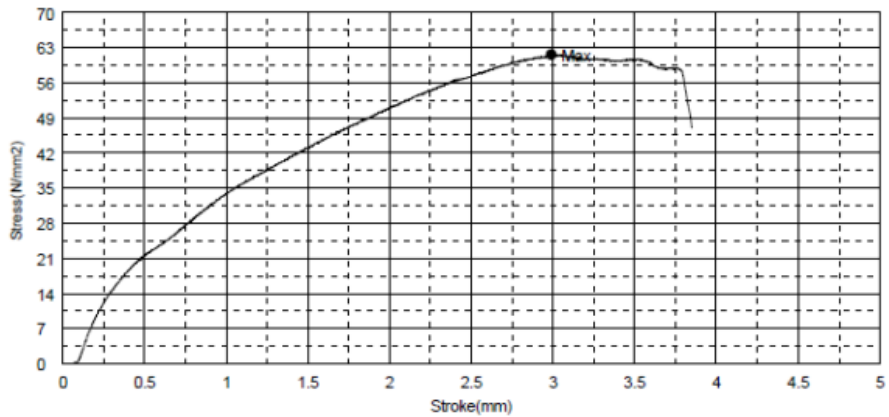


Fig. 6 Mg/Zn (3.10% Zn) Compression Strength Test graph.

In Fig. 7, the porosity, density, mass loss, pH and maximum stress values of the selected 3 implants with 0, 2.35 and 3.10% Zn contents are compared. It is seen that the difference in porosity changes is not very effective on pH and mass loss, but, it has a direct effect on compressive strength.

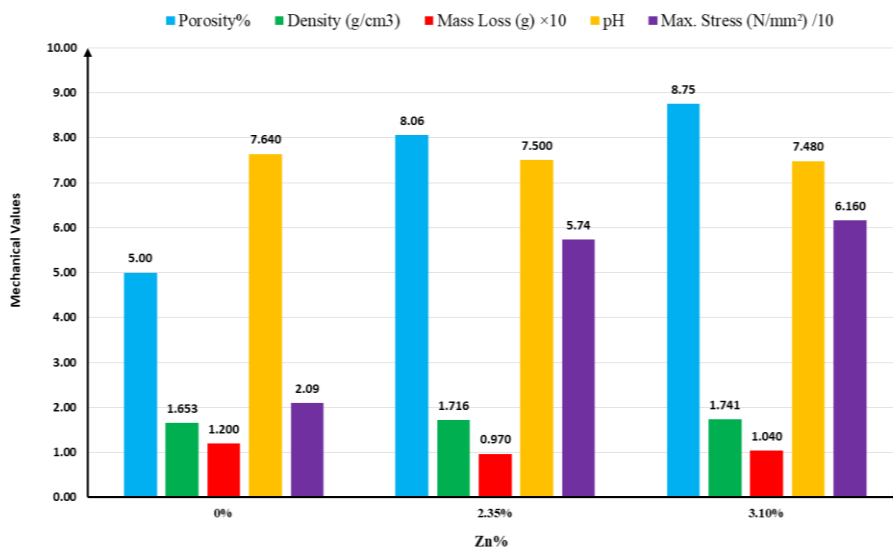


Fig. 7 Comparison of porosity, density of implants, mass loss and pH value changes in SBF solution for 3 selected implants (0%, 2.35% and 3.10%).

Table 5 (a), (e) and (i) show the images of Mg/MgO composites containing 0%, 2.35% and 3.10% Zn implants before placing them in the SBF solution. Images after corrosion in SBF solution of the same implants can be seen in Table 5 (b), (f) and (j). Mg/MgO composite deformation can be clearly observed.

The outer surface of the implant contains 3.10% Zn, as mentioned in pH measurement results. The increase in pH value of sample showed that this layer was $Mg(OH)_2$ with the support of information obtained from literature [21].

It was thought that this formed layer increased the resistance of the 3.10% Zn-containing implant in the SBF solution. The implant was thus able to remain intact at 192 hours in SBF solution. Although pH values were high during this period, they were not exposed to form any shape deformation.

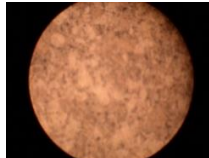
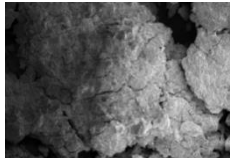
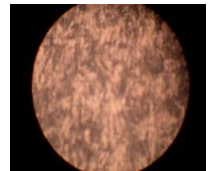
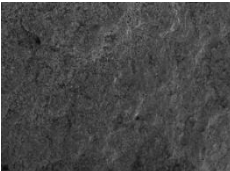
Table 5 (c), (g) and (k) show the optical microscope images. The implant containing 2.35% Zn showed a more homogenous distribution within the Mg structure. However, in the implant containing 3.10% Zn; Zn was found to be accumulated in some regions within Mg and thus homogeneous Zn distribution was not observed.

Finally, in Tables 5 (d), (h) and (l) are SEM images of implants containing Mg/MgO, 2.35% and 3.10% Zn content respectively. SEM images show why the strength of the composite Mg/MgO is shorter in the SBF solution compared to implants with a ratio of 2.35% and 3.10% Zn.

4. Conclusion

Mg implants with 7 different Zn content were produced by MA method. Mechanical tests and biodegradability of these alloys were carried out. The structural strengths of these 7 different implants, Mg ion concentration change in SBF, pH values and their compressive strength were examined.

Table 5 Visual observation of selected implant.

| %Zn Alloy | Sample Image | Sample Image After Corrosion in SBF | Optical Microscope image (100 μ m) | SEM image (100 μ m) |
|-----------|---|---|---|--|
| 0% |  |  |  |  |
| | (a) | (b) | (c) | (d) |
| 2.35% |  |  |  |  |
| | (e) | (f) | (g) | (h) |
| 3.10% |  |  |  |  |
| | (i) | (j) | (k) | (l) |

The aim of this study is to investigate the mechanism of bone-magnesium implant interaction and compare the relationship between different implants and different Zn% content of the degradation currently in use. Mg-Zn implants with different Zn contents were prepared by CIP method.

As a result of studies, following conclusive remarks are obtained:

- The implant with 2.35% Zn content had 360 hours and with 3.10% Zn had 192 hours of resistance. Among the produced implants, the most suitable preservation duration as 12-18 weeks can be achieved with Mg implants with the content of 2.35% and 3.10% Zn.
- When the change of Mg concentrations of the implants in the SBF solution given in Fig. 3 is examined, it is seen that the concentration values for all implants are generally increased. The mass change values given in Table 3 also indicate that the solution was absorbed by the implants and increase of mass was observed although ions were lost by implants.
- Mg implant with 2.35% Zn content is the longest lasting sample.
- The corrosion layer of all the magnesium alloys examined was in direct contact with the SBF solution during deterioration and it showed hydrogen gas accumulation (Fig.1).
- It was understood from the literature studies that the hydrogen gas (H_2) coming from the implants disrupts the hydronium (H^+) and Hydroxyl (OH^-) ion balance of the structure and therefore increases the pH value.
- Both implants with 2.35 and 3.10% Zn contents are recommended for further tests and studies.

Acknowledgement

This work was orally presented in the 4th International Symposium on Composites Materials (KOMPEGE 2018), 6-8 September, 2018, Izmir.

This study was financially supported by BAP 15-MÜH-069 project.

References

1. Friedrich HE. and Mordike BL. *Magnesium Technology: Metallurgy. Design Data. Applications* Berlin:Springer;2006.
2. Yuan X, Zhang J, Lian Y, Du C, Xu W, Zhao Y and Mo J. Research progress of residual stress determination in magnesium alloys review. *Journal of Magnesium and Alloys*, 2018;6:238-244.
3. Staiger MP, Pietak AM, Huadmai J and Dias G. Magnesium and its alloys as orthopedic biomaterials: a review. *Biomaterials*, 2006;27:1728-1734.
4. Fare S, Ge QA, Vedani M, Vimercati G, Gastaldi D and Migliavacca F. Evaluation of material properties and design requirements for biodegradable magnesium stents. *Materia-Brazil*, 2010;15:103-112.
5. Griebel AJ and Schaffer JE. Absorbable filament technologies: wire-drawing to enable next - generation medical devices. In: Singh A. et al. *Magnesium Technology 2016*. Berlin: Springer; 2016. p.323-327.
6. Mees SMD, Algra A, Wong GKC, Poon WS, Bradford CM, Saver JL, Starkman S, Rinkel GJE and Van Den Bergh WM. Early Magnesium treatment after aneurysmal subarachnoid hemorrhage individual patient data meta-analysis. *Stroke*. 2015;46:3190-3193.
7. Hermawan H, Dubé D and Mantovani D. Developments in metallic biodegradable stents. *Acta Biomater*, 2010;6:1693-1697.
8. Schaller B, Saulacic N, Imwinkelried T, Beck S, Liu EWY, Gralla J, Nakahara K, Hofstetter W and Iizuka T. In vivo degradation of magnesium plate/screw osteosynthesis implant systems: Soft and hard tissue response in a calvarial model in miniature pigs. *Journal of Cranio-Maxillofacial Surgery*, 2016;44:309-317.
9. Yu C, Wang C, Liu X, Jia XT, Naficy S, Shu KW, Forsyth M and Wallace GG. A cytocompatible robust hybrid conducting polymer hydrogel for use in a magnesium battery. *Advanced Materials*, 2016;28:9349-9355.
10. StJohn DH, Qian M, Easton MA, Cao P and Hildebrand Z. Grain refinement of magnesium alloys. *Metallurgical and Materials Transactions A*, 2005;36A:1669-1679.
11. He SM, Zeng XQ, Peng LM, Gao X, Nie JF and Ding WJ. Precipitation in a Mg- 10Gd-3Y-0.4Zr (wt.%) alloy during isothermal ageing at 250 °C. *Journal of Alloys and Compounds*, 2006;421:309-1313.
12. Witte F, Feyerabend F, Maier P, Fischer J, Stormer M and Blawert C. Biodegradable magnesium-hydroxyapatite metal matrix composites. *Biomaterials*, 2007;28:2163-2174.
13. Kannan MB and Raman RKS. In vitro degradation and mechanical integrity of calcium-containing magnesium alloys in modified-simulated body fluid. *Biomaterials*, 2008;29:2306-2314.
14. Erinc M, Sillekens WH, Mannens R and Werkhoven RJ. Applicability of existing magnesium alloys as biomedical implant materials. In: Warrendale, PA. *Minerals, Metals and Materials Society*, 2009; p.209-214.
15. Xu ZG, Smith C, Chen SO and Sankar J. Development and microstructural characterizations of Mg-Zn-Ca alloys for biomedical applications. *Materials Science and Engineering B*, 2011;176:1660-1665.

16. Poinern GEJ, Brundavanam S and Fawcett D. Biomedical magnesium alloys: a review of material properties, surface modifications and potential as a biodegradable orthopaedic implant. *American Journal of Biomedical Engineering*, 2012;2:218–240.
17. Zhao X, Shi LL and Xu J. Biodegradable Mg–Zn–Y alloys with long-period stacking ordered structure: optimization for mechanical properties. *Journal of the Mechanical Behavior of Biomedical Materials*, 2013;18:181–190.
18. Draxler J, Zitek A, Meischel M, Stranzl-Tschegg SE, Mingler B, Martinelli E, Weinberg AM and Prohaska T. Regionalized quantitative LA-ICP-MS imaging of the biodegradation of magnesium alloys in bone tissue. *Royal Society of Chemistry*, 2015;30:2459-2468.
19. Yuan X, Zhang J, Lian Y, Du C, Xu W, Zhao Y and Mo J. Research progress of residual stress determination in magnesium alloys review. *Journal of Magnesium and Alloys*, 2018;6:238–244.
20. Kokubo T and Takadama H. How useful is SBF in predicting in vivo bone bioactivity?. *Biomaterials*, 2006;27:2907–2915.
21. Wen CE, Yamada Y, Shimojima K, Chino Y, Hosokawa H and Mabuchi M. Compressibility of porous magnesium foam: dependency on porosity and pore size. *Materials Letters*, 2004;58:357–360.
22. Witte F, Hort N, Vogt C, Cohen S, Kainer KU and Willumeit R. Degradable biomaterials based on magnesium corrosion. *Current Opinion in Solid State and Materials Science*, 2008;12:63–72.
23. Zberg B, Uggowitz PJ and Loffler JF. MgZnCa glasses without clinically observable hydrogen evolution for biodegradable implants. *Nature Materials*, 2009;8:887-891.
24. Chen YJ, Li YJ, Walmsley JC, Dumoulin S, Skaret PC and Roven HJ. Microstructure evolution of commercial pure titanium during equal channel angular pressing. *Materials Science and Engineering A*, 2010;527:789–796.
25. Nakamura Y, Tsumura Y, Tonogai Y, Shibata T and Ito Y. Differences in behavior among the chlorides of seven rare earth elements administered intravenously to rats. *Fundamental and Applied Toxicology*, 1997;37:106–116.
26. Polmear IJ, Grades and alloys. In: Avedesian MM and Baker H. *ASM Speciality Handbook- Magnesium and magnesium alloys*. Materials Park, OH: ASM International Handbook Committee 1999; p.12–25.
27. Yang Z, Li JP, Zhang JX, Lorimer GW and Robson J. Review on research and development of magnesium alloys. *Acta Metallurgica Sinica (English Lett)*, 2008;21:313–328.
28. Purnama A, Hermawan H, Couet J and Mantovani D. Assessing the biocompatibility of degradable metallic materials: state-of-the-art and focus on the potential of genetic regulation. *Acta Biomaterialia*, 2010;6:1800-1807.
29. Bowen PK, Drelich J and Goldman J. Zinc exhibits ideal physiological corrosion behavior for bioabsorbable stents. *Advanced Materials*, 2013;25:2577–2582.
30. Brar HS, Keselowsky BG, Sarntinoranont M and Manuel MV. Design considerations for developing biodegradable and bioabsorbable magnesium implants. *JOM-US*, 2011;63:100–104.
31. Persaud-Sharma D and McGoron A. Biodegradable magnesium alloys: a review of material development and applications. *Journal of Biomimetics, Biomaterials and Tissue Engineering*, 2011;12:25–39.
32. Witte F, Fischer J, Nellesen J, Crostack HA, Kaese V and Pisch A. In vitro and in vivo corrosion measurements of magnesium alloys. *Biomaterials*, 2006;27:1013–1018.
33. Zhang XB, Yuan GY, Mao L, Niu JL and Ding WJ. Biocorrosion properties of as extrude Mg–Nd–Zn–Zr alloy compared with commercial AZ31 and WE43 alloys. *Materials Letters*, 2012;66:209–211.
34. Zhang SX, Zhang XN, Zhao CL, Li JA, Song Y and Xie CY. Research on an Mg– Zn alloy as a degradable biomaterial. *Acta Biomaterialia*, 2010;6:626–640.

35. Peng QM, Huang YD, Zhou L, Hort N and Kainer KU. Preparation and properties of high purity Mg–Y biomaterials. *Biomaterials*, 2010;31:398–403.
36. Persaud-Sharma D and McGoron A. Biodegradable magnesium alloys: a review of material development and applications. *Journal of Biomimetics, Biomaterials and Tissue Engineering*, 2011;12:25–39.